



## Structural Characterization of InSe:Zn Binary Semiconductor Grown by Bridgman/Stockbarger Technique

**Bekir Gürbulak**

*Department of Physics, Faculty of Sciences, Atatürk University*

**Afsoun Ashkhasi**

*Department of Physics, Faculty of Sciences, Atatürk University*

**Mehmet Şata**

*Department of Physics, Faculty of Sciences, Atatürk University*

**Fikriye Şeyma Özçelik**

*Department of Physics, Faculty of Sciences, Atatürk University*

**Songül Duman**

*Department of Basic Sciences, Faculty of Sciences Erzurum Technical University*

### ABSTRACT

Zn doped InSe (InSe:Zn) single crystal has been grown by using the Bridgman/Stockbarger method. There is no cracks or voids on the surface of ingots. Samples have been cleaved along the cleavage planes (001). The freshly cleaved crystals have mirror-like surfaces even without using mechanical treatment. The structure and lattice parameters of the InSe:Zn semiconductor has been analyzed using a X-ray diffractometer (XRD), Scanning electron microscopy (SEM) and energy dispersive X-rays (EDX) techniques. Zn doping causes a significant increase in the XRD peak intensity. It is found that the InSe:Zn crystal has hexagonal structure and calculated lattice constants are found to be  $a=b=5.845 \text{ Å}$  and  $c=16.788 \text{ Å}$  for InSe:Zn. The crystallite sizes have been calculated to be 42-155 nm for InSe:Zn crystal from the SEM results. The residual strain ( $6.16 \times 10^{-4} \text{ lin}^{-2} \text{m}^{-4}$ ) and dislocation density ( $2.98 \times 10^{15} \text{ lin m}^{-2}$ ) values have been calculated using powder XRD results (004), respectively. Zn doping causes a significant increase in the XRD peak intensity. The crystallite sizes have been calculated to be 50-125 nm for InSe:Zn from the SEM results. It has been observed from EDX results that InSe contains In=57.04 %, Se=38.46% and O=4.50%, respectively. These results are in a good agreement with the ones obtained from EDX analysis.

**Keywords:** InSe:Zn, single crystals, structural analysis.

### 1 INTRODUCTION

Binary semiconductor compounds have attracted the technological interest owing to their promises for practical application in the areas of visible and infrared light emitting diodes, infrared detectors, optical parametric oscillators, nonlinear optics, solar cells, optical frequency conversion, second harmonic generation devices and many other electro-optical devices. The characteristics of these crystals which are important for the Nano and optoelectronic technology will be explored in detail by analysing the all

obtained results. InSe:Zn binary semiconductor compounds was grown in our crystal growth laboratory by the Bridgman-Stockbarger method.

It is well known that the single crystals of  $A^{III}B^{VI}$  type compounds, in particular of Indium Selenide (InSe), crystallize in a layered structure where each layer contains two In and two Se close-packed sub layers in the stacking sequence Se–In–In–Se [1]. It is a layered semiconductor, which can be cleaved to yield high-quality surfaces and has been shown a new class of materials for solar energy conversion application. The bonding between two adjacent layers is of the weak Van der Waals type, while within the layer the bonding is predominantly covalent. Depending on the packing of the layers the indicated single crystals form various modifications, in which the positions of band edges are determined by interlayer interactions. Binary semiconductor compounds have attracted the technological interest owing to their promises for practical application in the areas of visible and infrared light emitting diodes, infrared detectors, optical parametric oscillators, nonlinear optics, solar cells, optical frequency conversion, second harmonic generation devices and many other electro-optical devices.

Although semiconducting compound thin films on conducting substrates have attracted much attention in recent years for the fabrication of solar cells and there are a number of deposition techniques such as vacuum evaporation [2], molecular beam epitaxy [3], flash evaporation [4], chemical vapor deposition [5], Van der Waals epitaxy [6] for the preparation of thin films [7]. The Bridgman/Stockbarger technique is an inexpensive, simple and low temperature growth method that could produce bulks of high quality for the device applications such as heterojunction devices with a very low interface density of states, switching devices and etc.

Balitskii et al [8] have used the methods of cathodoluminescence analysis and of X-ray diffraction (XRD) to study the chemical phase compositions of films [8]. Structural studies showed the presence of  $In_4Se_3$  with InSe [9]. X-ray diffraction spectrum reveals that the synthesized products were single-crystalline of the  $\beta$ -phase hexagonal structure of InSe with lattice constants  $a = 4.006 \text{ \AA}$  and  $c = 16.642 \text{ \AA}$ . The strong peak due to the reflection from the (004) crystal plane reveals that most nanowires grown with a strong preferred orientation [10]. The crystal structure of the  $\gamma$ - $In_2Se_3$  films was determined by X-ray diffraction and Raman spectroscopy in a study carried out by the Lyu et al, (2010). From the temperature dependence of the free exciton line, the room-temperature energy gap of  $\gamma$ - $In_2Se_3$  films is found to be about 1.947 eV [11]. Highly oriented InSe films has been prepared onto heated quartz substrates using the co-evaporation technique with 20% Se over pressure followed by 1 hour annealing at the growth temperature and have been characterized by XRD, Raman spectroscopy and atomic force microscopy [12]. In this study, undoped InSe and zinc (Zn) doped (InSe:Zn) single crystals belonging to the family of III-VI compound semiconductors and used for many technological applications have been grown and their structural and morphological analyses have been carried out at room temperature. They were prepared by Bridgman/Stockbarger method, starting from synthesized material with a stoichiometric content of In, Se and Zn of purity 99.999%. We present the results of the systematic studies on the optical, morphological and structural properties of the InSe:Zn. The structural and morphological characterization of the crystals were analyzed by means of XRD, energy dispersive X-rays (EDX) and scanning electron microscopy (SEM).

## 2 EXPERIMENTAL PROCEDURES

The horizontal furnace used in this work consists of two zones, each with an alumina tubes 50 cm in length as shown in figure 1. The furnace was heated using kanthal DSD (Cr-Al-Fe) heating elements. The temperature of each zone was monitored by K type (Cromel-Alumel) thermocouples positioned close to the middle of the zone. Two thermocouples were used to control the stability of temperature in the region of growth.

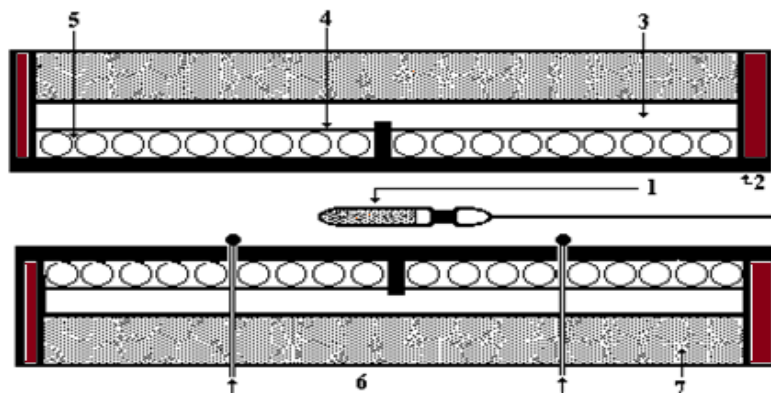


Figure 1: The horizontal furnace. 1. Quartz rod, 2. Alumina tube, 3. Zirconium blanket for insulation, 4. Aluminium foil, 5. Heating element (Cr-Al-Fe), 6. Thermocouples, 7. Air pocket.

For the constituent of polycrystalline  $A^{III}B^{VI}$ , the first important step in obtaining high quality crystals is the purity of the basic elements which are being involved in the structure. These elements were weighed in a stoichiometric ratio accurate to 0.1 mg. The total mass of the elements was about 40 g. The basic criteria for this choice were, firstly a sufficient need to justify the cost of one run, secondly minimal loss of the material in case of breakage.

The choice of a growth technique for a particular material depends on many factors which may be summarized as follows:

- The chemical reactivity of the compound and constituent the elements.
- The dissociation vapour pressure of the compound at the growth temperature.
- The melting point of the compound and whether the compound and whether the compound melts congruence or not.
- Presence or absence of phase transformations.

This stoichiometric ratio necessary to produce 40 g InSe:Zn was calculated using the following relationships:

$$M_{In} = (M_{Se} / A_{Se}) A_{In} \quad (1)$$

With total mass,

$$M_{In} + M_{Se} = 40 \text{ g} \quad (2)$$

Where,  $M$  and  $A$  are total and atomic masses, respectively.

The melting point of  $660 \pm 5$  °C [13] of the InSe compound were determined from the phase diagram. Sealed quartz ampoule was annealed at 1000 °C for 24 hours in the out gassing furnace designed in our laboratories. The temperature of quartz ampoule was decreased to room temperature in 24 hours. The mix In-Se and (0.01 wt % Zn) put into quartz ampoule and quartz ampoule was sealed under a vacuum of  $10^{-6}$  mbar. Quartz ampoules were coated with carbon. The crucible was suspended in the middle of the vertical furnace with two zone designed. Growth program of InSe:Zn single crystal has been given in Figure 2.

The following processes were applied for crystal. A sealed quartz ampoule was annealed at 1000 °C for 10 hours in the outgassing furnace. Then, it was ramped down to room temperature during a 7 hour period. The quartz ampoule was coated with carbon. The mixture of Se-In-In-Se-Zn (0.001 Zn) was put in it and sealed under a vacuum of  $10^{-6}$  mbar. The ampoule was suspended into the middle of the vertical furnace. The temperature of furnace was increased up to 150 °C and kept at that temperature for 4 hours and then heated up to 210 °C and kept for another 5 hours. It was further increased to 750 °C and kept for 40 hours. The temperature of furnace was increased to 750 °C and kept constant at this temperature for 120 hours. The zone having lower temperature rather than other zone was reduced to 550 °C at a rate of 6 °C /h.

Both of the furnace zones were cooled to 550 °C in 120 hours. The temperature of lower zone of furnace was reduced to 300 °C at a rate of 2.3 °C/h. Both of the furnace zones cooled to 300 °C in 130 hours. The solidified ingot was cooled to room temperature in 150 hours.

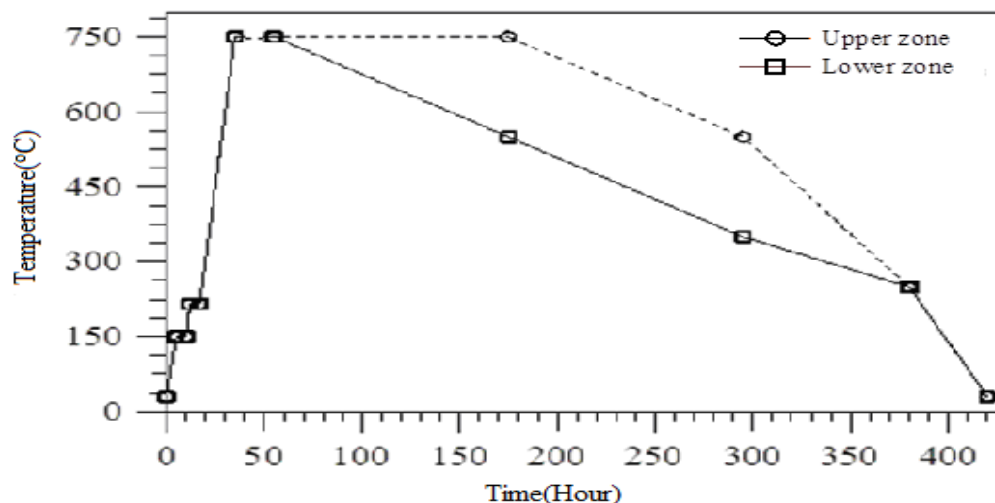


Figure 2: Growth program for InSe:Zn single crystal.

The prepared InSe:Zn single crystal ingot was 10 mm in diameter and about 50 mm in length. The ingot had no cracks or voids on the surface. No polishing or cleaning treatments were carried out on the cleaved faces of this sample because of the natural mirror-like cleavage faces. They were cleaved into perpendicular planes of naturally cleaved planes.

A<sup>III</sup>B<sup>VI</sup> compounds consist of two groups (III. group: Tl, Ga, In and VI. group: Se, S, Te): 1. GaSe, GaS and InSe have layered structure, and 2. TlGaSe<sub>2</sub>, TlGaTe<sub>2</sub> and TlGaSe<sub>2</sub> have a chained structure. The quartz ampoules, which are illustrated in Figure 3, have been formed according to the structure (layer chain) of growth crystals. Ampoules numbered 1, 2, 3, and 4 were used to grow layered structures (InSe, GaS and GaSe) and those numbered others 5, 6 and 7 were used to grow chained structures (TlInSe<sub>2</sub>, TlInTe<sub>2</sub> and TlGaTe<sub>2</sub>). The quartz ampoules used in the growth process were shaped and carbon coated in our crystal growth laboratory. The general procedure for cleaning the ampoules was follows:

- i. The ampoules were cleaned with diluted HNO<sub>3</sub> for four hours in order to remove metallic contamination on the surface.
- ii. Each was then rinsed repeatedly with deionised water.
- iii. Each was soaked in liquid jell for 30 hours and rinsed again with deionised water to remove dust particles or grease on the inner surface of the ampoule.
- iv. The inner and outer surface of the ampoules were etched with HF (45 % diluted) for 6 minutes to help further removal of any residual contaminations.
- v. The ampoules were once again rinsed with deionised water, washed with acetone and left to dry.
- vi. The ampoules in outgas furnace were baked at 1050 °C for 30 hours in order to outgas of them.
- vii. Each ampoule was ultrasonically washed in deionised water.

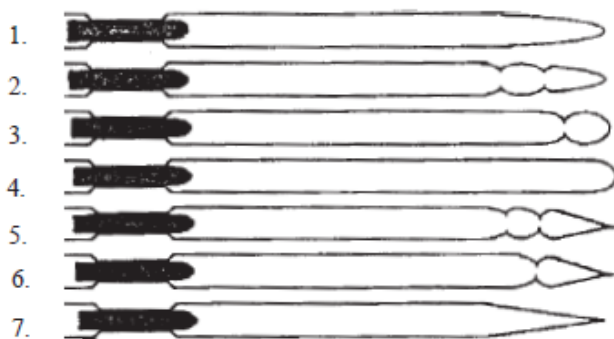


Figure 3: Typical ampoule shapes.

Since there is a temperature gradient along the synthesis ampoule, the melt solidifies directionally provides polycrystalline ingots (fig. 4). After optimization of solidification regime, a growth of single crystal is likely to be possible directly on the stage of post-synthesis cooling.



Figure 4: Synthesized material and grown crystals of InSe:Zn

The temperature of furnace is increased step by step paying attention to melting point of grown crystal and of using elements when the necessary temperature is obtained to grow crystals. The temperature of growth furnace is decreased to room temperature step by step paying attention to phase transition temperature. A schematic of the overall system is shown in Figure 5. The crystal growth system has continuous working characteristic, and has been controlled from both zones of the furnace. Temperature within the furnace was controlled via a Variac and the velocities (times) were controlled setting by a Temperature Control Unit (T.C.U).

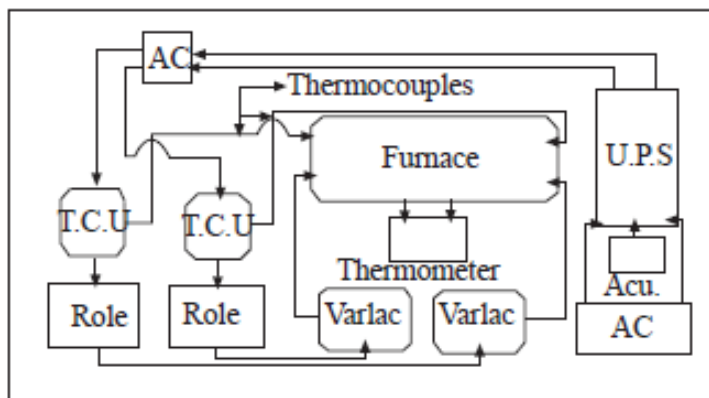


Figure 5: Schematic appearance of growth system. (T.C.U): Temperature Control Unit, (U.P.S): Uninterruptible Power Supply.

Zn doped InSe (InSe:Zn) single crystal was grown by using the Bridgman/Stockbarger method. The structural characterization of the single crystals deposited films were analysed by means of XRD, SEM and EDX measurements. The structural and lattice parameters of the InSe:Zn semiconductors were analyzed using a X-ray diffractometer (XRD) using Cu-K $\alpha$  radiation with a wavelength of  $\lambda=1.54050 \text{ \AA}$  (Rigaku Miniflex).

### 3 BASIC EQUATION

From the XRD profiles, the inter-planar spacing  $d_{hkl}$  was calculated for the (004) plane using the Bragg's relation [14].

$$d_{hkl} = \frac{n\lambda}{2 \sin \theta} \quad (3)$$

Where,  $\lambda=1.54056 \text{ \AA}$  is the wavelength of the X-ray radiation,  $d$  is the lattice spacing,  $n$  ( $n=1,2,3,..$ ) is the order number and  $\theta$  is the Bragg's angle. The factor  $d$  is related to ( $h k l$ ) indices of the planes and the dimension of the unit cells. The peak width at half maximum used to determine the crystallite size ( $D$ ) by using Debye–Scherrer formula is,

$$D = \frac{K\lambda}{(\beta \cos \theta)} \quad (4)$$

where  $K=0.94$  is the Scherrer constant,  $\beta$  is the full width at half maximum in radians and  $\theta$  is the Bragg diffraction angle. The strain ( $\epsilon$ ) value may be evaluated using the relation

$$\epsilon = \frac{(\beta \cos \theta)}{4} \quad (5)$$

The dislocation density ( $\delta$ ) may be calculated by using the formula [15].

$$\delta = \frac{15 \epsilon}{(aD)} \quad (6)$$

### 4 RESULTS AND DISCUSSION

Figure 6 shows the XRD pattern of the undoped InSe: Zn semiconductor. The values of  $2\theta$  were altered between 10 deg and 90 deg with the step of 0.1 deg/sec. It is found that the InSe:Zn crystals had

hexagonal structure, quite close  $2\theta$  peak values and dominant diffraction peak around  $2\theta = 22.29^\circ$  degrees for the both was the (004) plane.

This result is in a good agreement with that obtained by refs [16-24]. In addition to this (004) peak, some other peaks corresponding to (004), (002), (006), (008) (0010), (0012), (0014) [16;21;25], orientations were also observed. The results given in Figure 6 are in good agreement with those in the literature.

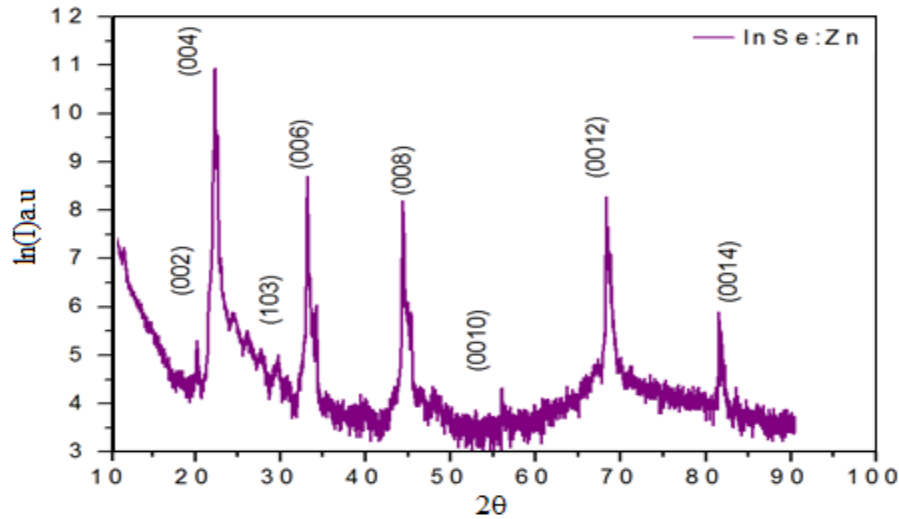


Figure 6: X-ray diffraction (XRD) spectra of InSe:Zn after annealing ( $T=300^\circ\text{C}$ ). The Miller indices are indicated on each diffraction peak.

The values of standard interplanar distance ( $d_0$ ) and observed interplanar distance ( $d_{\text{exp}}$ ) calculated by using Eq. (3) along with their respective planes for InSe:Zn semiconductor has been given in Table 1. As clearly seen from Figure 6 and from intensity ratio data given in Table 1, the XRD peak intensities decrease with Zn doping. It has been determined from Bragg diffraction law [26] that InSe crystals grown by Bridgman method had generally  $\gamma$ -polytype hexagonal structure.

Table 1 The standard and calculated XRD results for the InSe:Zn.

Peak	(hkl)	$2\theta$	Intensity	$d_{\text{exp}}$	$d_{\text{teo}}$	Structure
1	(002)	11.63	1370	7.63	7.60	Hexagonal
2	(004)	22.29	47421	4.068	4.060	Hexagonal
3	(103)	29.26	120	3.05	3.04	Hexagonal
4	(006)	33.23	6019	2.70	2.69	Hexagonal
5	(008)	44.39	3691	2.04	2.038	Hexagonal
6	(0010)	56.01	73.8	1.64	1.639	Hexagonal
7	(0012)	68.35	3882	1.376	1.371	Hexagonal
8	(0014)	81.56	363	1.18	1.17	Hexagonal

The crystallite size, dislocation density and residual strain for the InSe:Zn has been calculated using the Eq (4), Eq (5) and Eq (6), respectively. The analysis results obtained from EDX, SEM and XRD measurements has been presented in Table 2. The lattice parameter  $a$  and  $c$  of the hexagonal structure of InSe:Zn can be calculated using the following relation:



$$\frac{1}{d_{hkl}^2} = \frac{4}{3} \left( \frac{h^2 + hk + k^2}{a^2} \right) + \frac{l^2}{c^2} \quad (7)$$

Where (hkl) are the miller indices (004). The calculated lattice constants were found to be  $a=b=4.002 \pm 0.004 \text{ \AA}$  and  $c=17.160 \pm 0.004 \text{ \AA}$  for InSe and  $a=b=5.845 \pm 0.004 \text{ \AA}$  and  $c=16.788 \pm 0.004 \text{ \AA}$  for InSe:Zn. These values are almost agreed with the ones given in JPCDS card No.: 34-1431 ( $a=4.005 \text{ \AA}$  ve  $c=16.640 \text{ \AA}$ ). The number of crystallites per unit area (N) of the films was determined using the relation [27](where t is the thickness of the semiconductor crystal):

$$N = \frac{t}{D^3} \quad (8)$$

The surface morphology images of the InSe:Zn crystals were obtained by scanning electron microscope (SEM) technique at 15 kV with a 25.000 magnification. The surfaces of the InSe:Zn was coated with Au for SEM image enhancement. Figure 7 shows the SEM images of InSe:Zn crystals. It can clearly be seen that crystal has smooth and homogeneous surfaces.

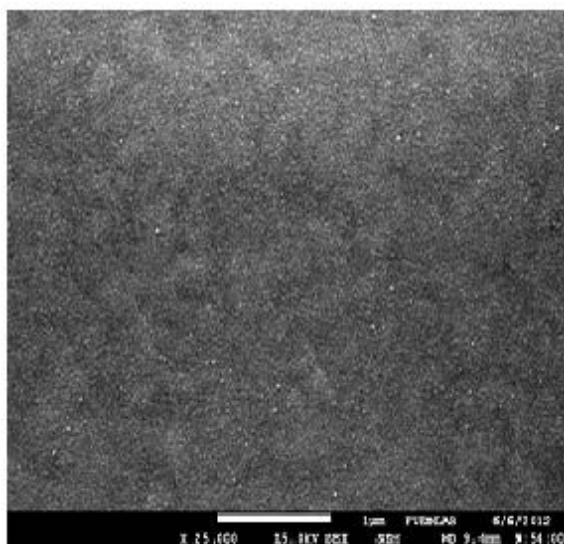


Figure 7: SEM images taken at 15 kV with a 25.000 magnification for InSe:Zn crystal.

It has been found that they have a novel hexagonal form and their crystallite sizes, being quite close to each other, have been calculated to be 50-125 nm for InSe:Zn. These results are in a good agreement with the ones obtained from EDX analyses. Figure 8 show the EDX spectra of InSe:Zn

Table 2 The crystallite size (D), dislocation density ( $\epsilon$ ) and residual strain ( $\delta$ ) for the undoped InSe and InSe:Zn.



Peaks	hkl	FWHM (deg)	D <sub>teo.</sub> (Å)	D <sub>exp.</sub> (Å)	$\varepsilon$ (lin <sup>-2</sup> m <sup>4</sup> ) x10 <sup>-4</sup>	$\delta$ , (lin/m <sup>2</sup> ) x10 <sup>14</sup>	N, (m <sup>-2</sup> ) x10 <sup>18</sup>
1	(002)	0.202	439.1	413.43	8.78	5.85	2.40
2	(004)	0.144	623.7	587.5	6.16	2.98	1.22
3	(103)	0.073	1246.4	1175.97	3.07	0.723	0.147
4	(006)	0.165	559.3	525.16	6.89	3.62	1.65
5	(008)	0.187	511.3	480.1	7.54	4.34	2.17
6	(0010)	0.048	2060.2	1980.8	1.84	0.260	0.0318
7	(0012)	0.073	1388.0	1375.0	2.64	0.528	0.0923
8	(0014)	0.084	1388.0	1307.22	2.77	0.585	0.1074

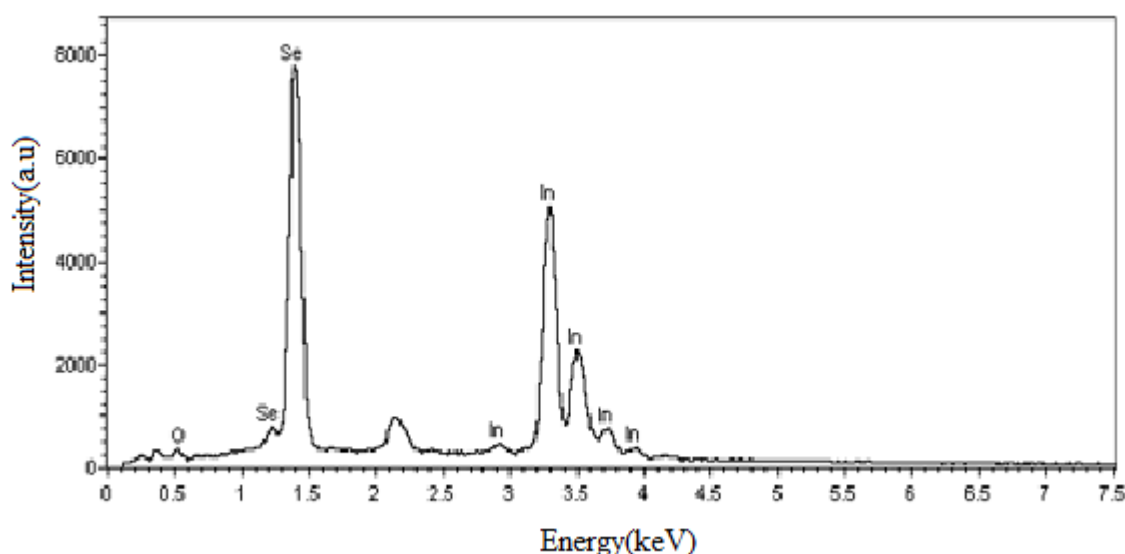


Figure 8: EDX spectra for InSe:Zn crystals.

The doping of Zn element with 0.01 percent into the InSe has not changed much the structure. In and Se elements have been taken as 61.17%, and 38.83% in order to obtain the stoichiometric ratio being an important issue for the constituent of InSe compound, respectively. However, according to the EDX results, InSe contains In=57.04 %, Se =38.46% and O= 4.50%, respectively. These values are quite close to the expected ones and a little amount of In has been got bonding with O.

## 5 CONCLUSION

InSe:Zn single crystal used in this research was grown by using the Bridgman/Stockbarger method. The ingots have no cracks and voids on the surface in ingots. There is no process to polish and clean treatments at cleavage faces of these samples because of the natural mirror-like cleavage faces. InSe has specific impurities arising from its crystal structure. When transition element doped in to InSe single crystals, these impurities which are transition elements are eliminated from the crystal during the growth process. Samples were cleaved along the cleavage planes (001). The freshly cleaved crystals had mirror-like surfaces even before using mechanical treatment.

The structure and lattice parameters of the InSe:Zn semiconductor has been analyzed using a X-ray diffractometer (XRD), Scanning electron microscopy (SEM) and energy dispersive X-rays (EDX) techniques. Zn doping causes a significant increase in the XRD peak intensity. It is found that the InSe:Zn crystal has hexagonal structure and calculated lattice constants are found to be  $a=b=5.845 \text{ \AA}$  and  $c=16.788 \text{ \AA}$  for InSe:Zn. The crystallite sizes has been calculated to be 42-155 nm for InSe:Zn crystal from the SEM results. The residual strain ( $6.16 \times 10^{-4} \text{ lin}^{-2} \text{m}^{-4}$ ) and dislocation density ( $2.98 \times 10^{15} \text{ lin m}^{-2}$ ) values have been calculated using powder XRD results (004), respectively. Zn doping causes a significant increase in the XRD peak intensity. The crystallite sizes have been calculated to be 50-125 nm for InSe:Zn from the SEM results. It has been observed from EDX results that InSe contains In=57.04 %, Se =38.46% and O=4.50%, respectively. These results are in a good agreement with the ones obtained from EDX analysis.

## 6 HIGHLIGHTS

1. Zn doped InSe (InSe:Zn) single crystals have been grown by using the Bridgman/Stockbarger method.
2. The structural was studied by employing
3. The techniques of XRD, SEM and EDX
4. XRD studies revealed that the prepared bulks were crystalline in nature.
5. SEM observation showed that the larger grains increased as the indium content in the bulk was increased
6. Zn doping of the InSe compound revealed new diffraction peaks.
7. The crystallite sizes have been calculated to be 50-125 nm for InSe:Zn from the SEM results.

## 7 ACKNOWLEDGEMENTS

This work was supported by the Atatürk University Research Fund, Project No: 2013/286

## REFERENCES

- [1] Mooser E. (1976). Physics and Chemistry of Material With Layered Structure
- [2] El-Sayed S. M. (2003). Vacuum. 72, 169–75.
- [3] Emery J. Y., Brahimotsmane L., Jouanne M., Julien C., and Balkanski M.(1989). Mat. Sci. Eng. B, 3, 13–17.
- [4] Julien C., Benramdane N. and Guesdon J. P.(1990). Semicond. Sci. Technol 5, 905–10.
- [5] Park J., Fzaal M. A., Helliwell M., Malik M. A., Obrien P. and Raftery J. (2003). Chem. Mater, 15, 4205–10.
- [6] Lang O., Klein A., Pettenkofer C. and Jaegermann W.( 1996). J. Appl. Phys 80, 3817–21.
- [7] Ohring M.(1992). The Materials Science of Thin Films, Academic press (Boston, MA)
- [8] Balitskii O. A., Lutsiv R. V., Savchyn V. P. and Stakhira J. M. (1998). Materials Science and Engineering B, 56, 5–10.
- [9] Kobbi B., Ouadjaout D. and Kesri N. (2001). Vacuum 62, 321-24.
- [10] Siciliano T., Tepore A., Micocci G., Genga A., Siciliano M. and Filippo E. (2011). J Mater Sci Mater Electron, 22, 649–53.

- [11] Lyu D., Lin T. Y., Chang T. W., Lan S. M., Yang T. N., Chiang C. C., Chen C. L. and Chiang H. P.( 2010). Journal of Alloys and Compounds, 499, 104–07.
- [12] Hirohata A., Moodera J. S. and Berera G.P.( 2006). Thin Solid Films, 510, 247–50.,
- [13] Imai K., Haga T., Hasegawa Y. and Abe Y.( 1981) J. Cryst. Growth, 54, 501-06.
- [14] Cullity B. D.(1972). Elements of X-Ray Diffraction, Addison Wesley, Reading, MA, 102
- [15] Abdullah M. M., Bhagavannarayana G. and Waha M. (2010). Journal of Crystal Growth, 312, 1534–37.
- [16] Hirohata A., Moodera J. S. and Berera G. P.( 2006). Structural and electrical properties of InSe polycrystalline films and diode fabrication. Thin Solid Films, 510, 247-250.
- [17] Siciliano T., Tepore A, Micocci G., Genga A., Siciliano M. and Filippo E.( 2011). Synthesis and characterization of indium monoselenide (InSe) nanowires. J Mater Sci: Mater Electron 22, 649–653.
- [18] Gysling H. J., Wernberg A. A. and Blanton T. N.(1992). Molecular Design of Single- Source Precursors for 3-6 Semiconductor Films 4, 900-905.
- [19] Choi I. and Yu P.Y. (2003). Properties of phase-pure InSe films prepared by metalorganic chemical vapor deposition with a single-source precursor. Journal of Applied Physics, 93 (8), 4673-4677
- [20] Siciliano T., Tepore A, Micocci G., Genga A., Siciliano M. and Filippo E.( 2011). Synthesis and characterization of indium monoselenide (InSe) nanowires. J Mater Sci: Mater Electron, 22, 649–653.
- [21] Viswanathan C., Gopal S., Thamilselvan M., Premnazeer K., Mangalaraj D., Narayandass S. K., Yi J. and Ingram D.C.( 2004). Space charge limited current, variable range hopping and mobility gap in thermally evaporated amorphous InSe thin films. Journal of Materials Science: Materials in Electronics, 15, 787-792.
- [22] Viswanathan C., Senthilkumar V., Sriranjini R., Mangalaraj D., Narayandass S. K. and Yi J.(2005). Effect of substrate temperature on the properties of vacuum evaporated indium selenide thin films, Cryst. Res. Technol, 40 (7), 658 – 664.
- [23] Ateş A., Kundakçı M., Astam A., and Yıldırım M. (2008). Annealing and light effect on optical and electrical properties of evaporated indium selenide thin films. Physica E, 40, 2709-2713.
- [24] Siciliano T., Tepore A., Micocci G., Genga A., Siciliano M. and Filippo E. ( 2011). Formation of In<sub>2</sub>O<sub>3</sub> Microrods in Thermal Treated InSe Single Crystal. Crystal Growth Design, 11, 1924-1929.
- [25] Mosca D. H., Mattoso N., Lepienski C.M., Veiga W., Mazzaro I., Etgens V.H. and Eddrief M. (2002). Mechanical properties of layered InSe and GaSe single crystals. Journal of Applied Physics, 91 (1), 140-144
- [26] Zolfaghari M., Jain K. P., Mavi M. S., Balkanski M., Julien C. and Chevy A. (1996). Materials Science Engineering: B, 38, 161-70.
- [27] Ravichandran K., Sakthivel B. and Philominathan P.( 2010). Cryst. Res. Technol, 45, 292–98.